Indian Journal of Chemistry
Vol. 58A, October 2019, pp. 1075-1084

A novel electrochemical sensor based on Co_3O_4-CeO_2-ZnO multi metal oxide nanocomposite for simultaneous detection of nanomolar Pb^{2+} and Hg^{2+} in different kind of spices

Shahnaz Davoudi, Mohammad Hadi Givianrad*, Mohammad Saber-Tehrani & Parviz Aberoomand Azar
Department of Chemistry, Science and Research Branch, Islamic Azad University, Tehran, Iran
Email: givianradh@yahoo.com

Received 9 February 2019; revised and accepted 24 September 2019

Simultaneous and individual determination of Pb^{2+} and Hg^{2+} ions have been carried out based on the synergistic effect of Co_3O_4, CeO_2 and ZnO nanoparticles onto the carbon paste electrode. The morphology of synthesized nanocomposite (Co_3O_4-CeO_2-ZnO) has been investigated by Scanning Electron Microscope, Transmission Electron Microscope, X-ray diffraction and Fourier Transform Infrared spectroscopy. The voltammetric current has been increased linearly by increasing the concentration of Pb^{2+} and Hg^{2+} ions. The linear ranges of the Co_3O_4-CeO_2-ZnO/CPE sensor have been obtained 0.27–18.42 nM (for Pb^{2+} ions) and 0.42–31.30 nM (for Hg^{2+} ions), under optimum condition. The detection limits ($3S_b/m$) have been obtained 0.054 nM for Pb^{2+} and 0.097 nM for Hg^{2+}, respectively. The proposed electrochemical sensor acts as a sensitive and selective method for simultaneous determination of two heavy metal ions and shows excellent repeatability, reproducibility, and stability, with relative standard deviation (RSD) less than 3%. Finally, Co_3O_4-CeO_2-ZnO/CPE has been successfully applied for the determination of Pb^{2+} and Hg^{2+} in different kind of spices.

Keywords: Electrochemical determination, Modified electrode, Co_3O_4-CeO_2-ZnO, Multi-metal oxide: Pb^{2+}, Hg^{2+}

In the last decade, some electrochemical sensors have been developed using several kinds of functional materials to improve selectivity, stability and the sensor response. The electrochemical sensors have been modified by functional materials. Theses material included various nano-materials such as metal nanoparticles (NPs), metal oxide NPs, polymeric NPs, carbon-based nanomaterials and quantum dots[1-5]. A wide variety of nanocomposites have been recently applied to fabricate the modified sensors because of their biological compatibility, high-specific surface area, chemical stability, excellent catalytic activity and conductivity[6-13]. These nanocomposites including metal oxide NPs and multi-metal oxide nanocomposites have been utilized as catalysts owing to their unique electronic structure. Hence, the synthesis of metal oxide nanocomposites has been investigated in order to evaluate their performance in different applications such as fuel cells, super capacitors, and electrochemical sensors[14-16].

Cobalt oxide (Co_3O_4) has recently aroused considerable interest due to the normal spinel structure owing to some advantages including energy conversion, storage, electrocatalytic properties, magnetic properties, high theoretical specific capacitance, low cost and low toxicity[17,18]. In order to improve the electrochemical efficiencies of sensors, various nanostructures and synthesis of Co_3O_4 based material as a multi-metal oxide have been investigated[19,20]. Cobalt oxide (Co_3O_4) is very attractive for oxidation catalysts' preparation because of the presence of mobile oxygen in Co_3O_4. This means that the Co–O bond strength of Co_3O_4 is relatively weak, so reactive oxygen can be easily obtained from the lattice oxygen[21,22].

Cerium dioxide (CeO_2) NPs is one of the most interesting rare earth oxides. It is used in many chemical processes as an efficient catalyst and electronic booster, because of its high specific surface area, high conductivity, excellent redox performance, good mechanical strength and low-cost synthesis[23,24]. Ceria has a high oxygen storage capacity and well-known catalytic and redox properties (couples of Ce^{4+}/Ce^{3+}), making more oxygen available for the oxidation process. The most important property is the oxygen storage and releasing capacity of CeO_2[25]. In addition, the catalytic activity and electrochemical application of CeO_2 can be improved by mixing it with some metal oxides or metals[26,27].

Zinc oxide (ZnO) is a metal oxide NPs. It is a good electron acceptor with high electron mobility. It can be used as an appropriate conducting layer[28]. Zinc oxide nanoparticles have gained their attraction as adsorbents for heavy metals due to their high surface area, low cost and extraordinary removal capacity[29]. It is known that there are many hydroxyl groups on the surface of ZnO NPs, resulting in coordination interaction between heavy metal ions and hydroxyl groups, so ZnO NPs can be used as the adsorbents of heavy metal ions. However, the poor conductivity of ZnO has limited its application in electrochemistry[30].

The synergetic effects of composite nanomaterials can differentiate their catalytic performance from each one of the components. The composition and morphology of metal oxide NPs are controllable, and the lattice matching between metal oxides can be easily realized. Thus, metal oxides are suitable for support matrices. Several kinds of nanocomposites have been synthesized with two or three different metal oxide NPs, which have high specific surface area and catalytic activity[31,32]. Recently, the novel properties of multi-metal oxides nanocomposites have been considered which are suitable for microelectronic devices, catalyst and semiconductor devices[31,32,33]. There are many types of research carried out for the synthesis of bimetal-oxide nanocomposites such as Co_3O_4-CeO_2, CeO_2-ZnO, Co_3O_4-ZnO, and ternary metal oxide nanocomposites such as Co_3O_4-CeO_2-ZnO[33].

According to the previous studies, heavy metal ions are not biodegradable, so these ions remain in the ecological systems and food chain indefinitely. Among heavy metal ions, mercury (Hg^{2+}) and lead (Pb^{2+}) are well-known as toxic pollutants in the environments and ecosystems. Even low level of Hg^{2+} and Pb^{2+} lead to cancer, nervous disease, kidney damage, reproductive toxicity, birth defects and skin rash[34,6,7]. Owing to the wide usage of Hg^{2+} and Pb^{2+}, these are some of the causes of worldwide environmental pollution[35].

According the stated reasons, a simple and rapid detection of Hg^{2+} and Pb^{2+} is important in different types of real samples. There are different methods for individually and simultaneously determining of heavy metals including flame atomic absorption spectrometry[36], UV-vis spectrometry[37], electrothermal atomic absorption spectrometry[38], inductively coupled plasma atomic emission spectrometry (ICP-AES)[39], inductively coupled plasma mass spectrometry (ICP-MS)[40] and also electrochemical methods such as anodic stripping voltammetry (ASV)[41,6].

Among the stated analytical methods, the electrochemical methods and specially ASV have been accepted as one of the best methods for individually and simultaneously determining of heavy metal ions. This method has some advantages such as high sensitivity, selectivity, short analysis time, portability, low detection limit, simple fabrication and modification of working electrode[6,7]. The fabrication of various mercury-free electrodes and their modification using different materials to improve the surface area, conductivity, selectivity and sensitivity of electrode has been carried out over the past years. The applications of carbon paste electrode (CPE) as a working electrode for determination of different analytes has increased significantly owing to its low cost, easily fabrication, flexible substrate for modification, high sensitivity and renewable surface[13,42,43].

Earlier reports demonstrated that SnO_2/graphene composite modified on glassy carbon electrode could simultaneously detect some heavy metal ions[44]. However, anodic stripping voltammetry helped in simultaneous detection of heavy metal ions, it was bounded in terms of detection limit, sensitivity and relative correlation co-efficient. This was owing to the competition of Cd(II), Pb(II), Cu(II) and Hg(II) ions towards the limited number of active sites. Mafa *et al.,*[45] accomplished a bismuth film on the surface of electrode by electrodeposition of bismuth onto an EG electrode and used it for the co-detection of As(III), Hg(II) and Pb(II). The benefit that resulted was the inhibiting any damages of electrode's film and it could be used for electrochemical and other analytical tests.

Liu *et al*.,[46] prepared a ZnO NFs-coated GCE, with Nafion acting as an adhesive, and applied it as a new sensor for heavy metal determination with SWASV. The graphene/CeO_2 hybrid nanocomposite used in the development of modified electrodes for the simultaneous determination of Cd(II), Pb(II), Cu(II), and Hg(II) through differential pulse anodic stripping voltammetry (DPASV)[47]. An electrochemical sensor based on the use of CeO_2 nanoparticles modified glassy carbon electrode (CeO_2/GCE) was prepared and applied individually and simultaneously for the determination of Cu(II) and Hg(II). The DPASV results indicated that the CeO_2 NPs based sensor exhibits good electroanalytical performance with two well-resolved voltammetric stripping peaks for Cu(II) and Hg(II)[48]. A sensitive Pb(II) sensor was also fabricated based on Co_3O_4/reduced graphene oxide/chitosan (Co_3O_4/rGO/

chitosan) nanocomposite modified glassy carbon electrode (GCE). The Co_3O_4/rGO material was synthesized through in situ growth of Co_3O_4 nanoparticles (NPs) on GO and subsequent hydrazine reduction process[49]. An electrochemical platform for the detection of Pb(II) using porous Co_3O_4 microsheets was also introduced by Huang *et al*[50].

In this paper, a selective sensing electrode has been introduced based on Co_3O_4-CeO_2-ZnO/CPE for the individually and simultaneously determination of Hg^{2+} and Pb^{2+} ions in different kind of real samples.

Experimental

Chemicals and apparatus

All reagents were of analytical grade and used as received without any further purification. All of the working solutions were prepared using double distilled water (DDW). Laboratory glassware were kept overnight in a 10% (v/v) HNO_3 solution and then rinsed with DDW. Graphite powder (10 μm average particle size) and pure paraffin oil were purchased from Merck. $Co(NO_3)_2{\cdot}6H_2O$, $Zn(NO_3)_2{\cdot}6H2O$, $Ce(NO_3)_3{\cdot}6H_2O$ and Na_2CO_3 were purchased from Merck company and used in order to synthesise Co_3O_4-CeO_2-ZnO nanocomposite. Stock solutions of Pb^{2+} and Hg^{2+} (1000 mg L^{-1}) were prepared by dissolving appropriate amounts of $HgCl_2$ and $PbCl_2$ (Merck) in DDW, respectively. Britton-Robinson (B-R) buffers (pH 2–7) were prepared and they were tested as supporting electrolytes. Different real samples were purchased from the local market.

Behpajoh potentiostat/galvanostat system (Model BHP-2065-Iran) was used for all the electrochemical experiments. The electrochemical cell was assembled with a conventional three-electrode system A platinum wire, an Ag/AgCl/KCl (3 mol L^{-1}) electrode, modified or unmodified CPEs were employed as an auxiliary electrode, a reference electrode and working electrodes, respectively. The prepared nanocomposite was characterized by TEM images (Zeiss EM902A), XRD (38066 Riva, d/G. Via M. Misone, 11/D (TN)) and FT-IR (Perkin-Elmer, spectrum 100, FT-IR spectrometer). pH adjustments were carried out using a Metrohm model 713 (Herisau, Switzerland) pH-Meter.

Preparation of Co_3O_4-CeO_2-ZnO nanocomposite and Co_3O_4, CeO_2 and ZnO nanoparticles

The Co_3O_4-CeO_2-ZnO tri-metallic nanocomposite was synthesized by co-precipitation procedure. In the first step, the solution of $Co(NO_3)_2{\cdot}6H_2O$ and $Zn(NO_3)_2{\cdot}6H_2O$ (each of the solution was 0.25 M) were mixed in a 1:1 molar ratio and stirred for 2 h at room temperature. In the next step, the solutions of 0.25 M $Ce(NO_3)_3{\cdot}6H_2O$ and Na_2CO_3 (1 M) by same molar ratio were added to the previous solution. The solution was stirred for 3 h at room temperature. Finally, the precipitate was separated by centrifuge and washed by DDW. The obtained precipitate was dried in an oven at 90 °C for 1 h and at 200 °C for 3 h, respectively. To achieve the Co_3O_4-CeO_2-ZnO tri-metallic nanocomposite, the dried precipitate was sintered in a furnace at 450 °C for 5 h. In this stage, the nanocomposite was annealed at 950 °C for 10 h to convert carbonate to oxide sample. The Co_3O_4, CeO_2, and ZnO nanoparticles were also synthesized by the same method without addition of other ions.

Sensor preparation

The bare CPE was prepared by hand-mixing of a pure graphite powder and a certain amount of paraffin oil (ratio of 70:30 w/w) in an agate mortar.

To prepare the Co_3O_4-CeO_2-ZnO/CPE modified electrode, a 10% w/w portion of Co_3O_4-CeO_2-ZnO was mixed with 60% w/w graphite powder. It was dispersed in dichloromethane to well-mixing of the composite and was stirred until dichloromethane evaporated completely. Then the paraffin oil (30 % w/w) was added and mixed until the uniform paste was obtained. This paste preparation method was applied to provide a reproducible sensor after each surface polishing of the electrode. All amount of each paste was transferred into an insulin syringe and packed carefully to avoid possible air gaps and improve the electrode resistance. A copper wire (1.0 mm diameter) was inserted into the unmodified and modified electrode to establish the electrical contact.

Analytical procedure

Square wave anodic stripping voltammetry (SWASV) technique was used for determination of analytes under optimized condition. It was performed in a 20 mL electrochemical cell containing B-R buffer as a supporting electrolyte medium. Hg^{2+} and Cd^{2+} were deposited at the reduction potential of –0.75 V *vs.* Ag/AgCl for 110 s. Re-Oxidation of Pb^0 to Pb^{2+} and Hg^0 to Hg^{2+} were performed in anodic stripping step in the potential range of –0.8 to 0.5 V *vs.* Ag/AgCl. Before any measurement, in pre-conditioning step, a potential of 1.0 V *vs.* Ag/AgCl for 60 s was performed to ensure dissolution of the remaining deposits on the surface of Co_3O_4-CeO_2-ZnO/CPE. The pre-concentration and cleaning steps were done while the solution of the electrochemical cell was stirred. The peak currents were measured at potentials of about –0.41 and 0.18 V *vs.* Ag/AgCl for Pb^{2+} and Hg^{2+}, respectively.

Samples preparation

The proposed method was applied for the determination of Pb^{2+} and Hg^{2+} in 22 different spices samples. The sample preparation was performed based on standard methods of Institute of Standards and Industrial Research of Iran. Each sample was individually milled and sifted. About 0.50 g of the samples were incinerated for 5 h at 500 °C in a crucible. After cooling, the incinerated sample was carefully moistened with 12 mL of concentrated nitric acid. The mixture was heated on a hotplate for 5 min and filtered through filter paper. The filtration was collected into a 50 mL volumetric flask and diluted to the mark with DDW[31].

Results and Discussion

Characterization of synthesized nanocomposite

The morphology, structure, and size of synthesized materials were investigated by SEM and TEM. The SEM and TEM image of Co_3O_4-CeO_2-ZnO are shown in Fig. 1a and Fig. 1b, respectively. It is found that Co_3O_4-CeO_2-ZnO tri-metallic nanocomposite with the average size of about 17 nm (nanoparticles with diameters in the range of 8–25 nm) was synthesized by the co-precipitation procedure. It is noticeable that the synthesized method is efficient to prevent the aggregation of Co_3O_4, CeO_2, and ZnO nanoparticles. Hence, the synthetized nanocomposite has a high specific surface area.

To confirm the chemical structure of the synthesized nanocomposite, the FT-IR spectra of the Co_3O_4-CeO_2-ZnO tri-metallic nanocomposite (Fig. 1c) was recorded. The FT-IR spectrum of the nanocomposite illustrates the absorption band at about 3500, 1400, 1100, 1000, 820, 615 and 460 cm^{-1} which confirm the presence of O-H of the carboxylic groups, CO_3^{2-}, C-O, O-H, Ce-O, Zn-OH, and Zn-O. This absorption bands indicate the effectively synthesis of Co_3O_4-CeO_2-ZnO multi-metallic nanocomposite.

The XRD patterns of Co_3O_4-CeO_2-ZnO nanocomposite, Co_3O_4, CeO_2 and ZnO nanoparticles are shown in Fig. 1d. The XRD pattern of Co_3O_4 shows three peaks about 2θ = 31.77°, 36.28° and 56.42° which matches well with the standard sample

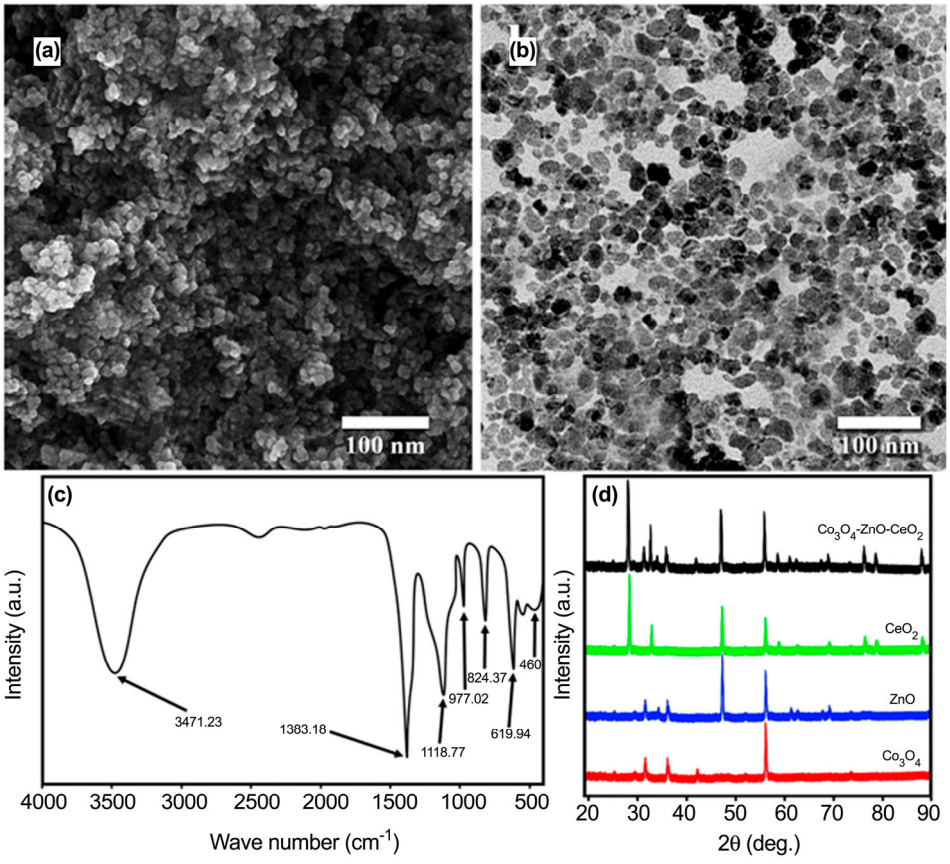

Fig. 1 — (a) SEM, (b) TEM, (c) FT-IR spectra of Co_3O_4-CeO_2-ZnO tri-metallic nanocomposite, and (d) XRD patterns of Co_3O_4, CeO_2, ZnO and Co_3O_4-CeO_2-ZnO nanocomposite.

(JCPDS-ICDD 9-418). The XRD pattern of the Co_3O_4 nanoparticles illustrate some peaks about 2θ = 28.5°, 33.09°, 47.46°, 56.42°, 59.10°, 69.37°, 79.13°, 76.79° and 88.55° which is matched with the standard sample (JCPDS-ICDD 43-1002). The XRD pattern of ZnO nanoparticles represents seven peaks about 2θ = 31.77°, 34.27°, 36.26°, 47.46°, 56.42°, 62.99° and 69.10°, which are adjusted with the standard sample (JCPDS-ICDD 36-1451). According to the obtained results of XRD pattern of Co_3O_4-CeO_2-ZnO tri-metallic nanocomposite, the positions of diffraction peaks are in agreement with the standard samples of Co_3O_4, CeO_2 and ZnO nanoparticles[30].

Voltammetric behavior of Pb^{2+} and Hg^{2+} on the surface of unmodified and modified electrodes

To explain the function of modifiers in the electrodes preparing process, the stripping voltammograms were recorded with different electrodes. Square-wave voltammograms of a solution containing 5.00 nM Pb^{2+} and Hg^{2+} in B-R buffer (pH = 4.5, 0.1M) at the bare CPE and Co_3O_4-CeO_2-ZnO/CPE by accumulation potential −0.75 V for 110 s in the potential range −0.8 to 0.5 V *vs.* Ag/AgCl are shown in Fig. 2.

Voltammograms of the solution at bare CPE exhibited no stripping peaks in used condition. After modifiying the sensing layer of electrode with Co_3O_4-CeO_2-ZnO nanocomposite, the Co_3O_4-CeO_2-ZnO/CPE did not show any oxidation peak in the absence of the analytes. After adding each analyte, two distinct stripping peaks can be seen for Pb^{2+} at –0.404 and Hg^{2+} at 0.183 V with the peak separation of 0.578 V *vs.* Ag/Ag/Cl. This peak was attributed to facilitating electron transfer between Pb^{2+} or Hg^{2+} ions and Co_3O_4-CeO_2-ZnO/CPE. It is also owing to increasing of the surface area of the electrode. Based on these observations, the Co_3O_4-CeO_2-ZnO/CPE can be useful for determination of Pb^{2+} and Hg^{2+} ions in aqueous solution.

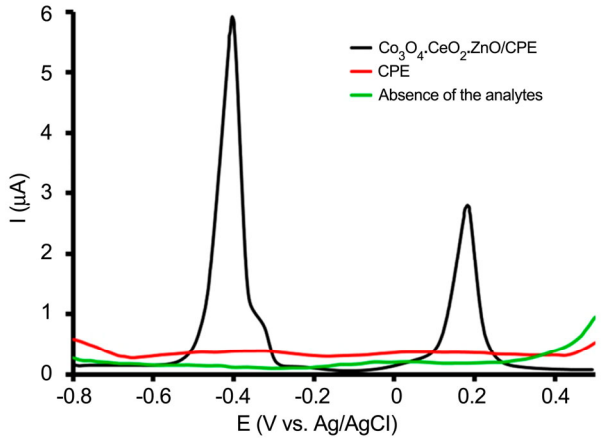

Fig. 2 — SW voltammograms in the absence and present 5.00 nM of Pb^{2+} and Hg^{2+}, on the surface of bare CPE, and Co_3O_4-CeO_2-ZnO/CPE.

The response of modified electrode is dependent on many factors including pH of solution, accommodation potential, time, and the instrumental parameters of SWV. These parameters were optimized to achieve the best peak shape, maximum current, and the lowest detection limit.

Effect of pH on the response of modified electrode

The effect of pH on the current responses of 5.00 nM of Pb^{2+} and Hg^{2+} on the Co_3O_4-CeO_2-ZnO/CPE was investigated in the range of 2.0 to 7.0 by SWV. The results are shown in Fig. 3a. The stripping currents for the both analytes have been raised by increasing of pH upto 4.5 and the maximum oxidation peak current appeared at pH 4.5. The peak current was decreased by further increasing of pH; it may be owing to the ions hydrolysis. Hence, the pH of 4.5 was selected for subsequent experiment[31,6].

Effect of deposition potential, deposition time and instrumental parameters on the voltammetric currents

Sensitivity and detection limit depend on deposition potential, accumulation time and instrumental parameters hence optimization of these parameters is necessary.

The effect of deposition potential on the stripping response of 5.00 nM Pb^{2+} and Hg^{2+} ions were studied while the deposition potential was changed from −0.6 and −0.9 V *vs.* Ag/AgCl on Co_3O_4-CeO_2-ZnO/CPE under optimimum conditions (Fig. 3b). The study represents that the electrode response increase gradually by changing the deposition potential upto –0.85 V *vs.* Ag/AgCl and accumulation time upto 110 s. On the other hand, the stripping responses for the both cations have decreased while the deposition potential was more negative than –0.85 V *vs.* Ag/AgCl, because of the reduction of other chemicals at these potentials. The hydrogen evolution was also started at such negative potentials. The background current was more than the other potential range. Hence, the potential of –0.85 V *vs.* Ag/AgCl was selected as an optimum deposition potential[6].

The effect of deposition time on the stripping responses of Pb^{2+} and Hg^{2+} ions was studied from 20 to 130 s with a deposition potential of –0.85 V, and it has been found that the oxidation response is increased by increasing of accumulation time up to

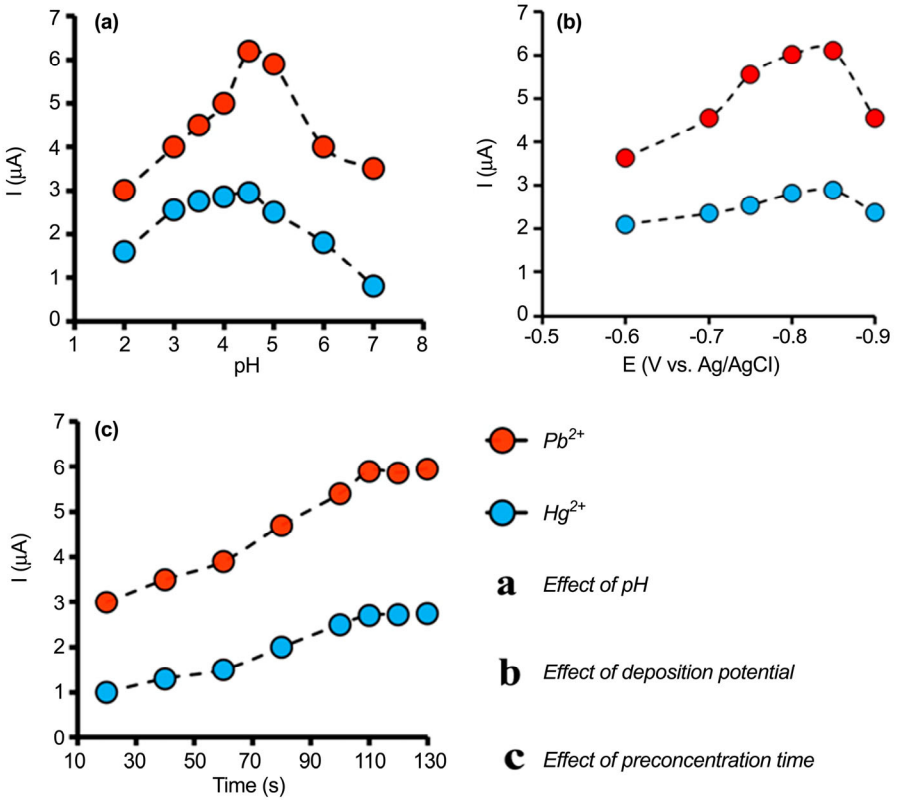

Fig. 3 — (a) Effect of pH on the on the voltammetric currents for 5.00 nM Pb^{2+} and Hg^{2+} solution. (b) Effect of deposition potential on the voltammetric currents for 5.00 nM Pb^{2+} and Hg^{2+} solution in pH = 4.5. (c) Effect of deposition time on the voltammetric currents for 5.00 nM Pb^{2+} and Hg^{2+} solution in pH = 4.5.

110 s (Fig. 3c). This is owing to the fact that the longer collection time caused more Pb^{2+} and Hg^{2+} ions to get accumulated at the electrode/solution interface onto modified surface, hence current increases. It can be seen that after 110 s, the stripping currents becomes approximately constant owing to surface saturation[6,7,51]. Hence, the accumulation time of 110 s was selected and used as an optimum condition.

In order to obtain well-defined SWASV peaks and the best response, the voltammetric instrumental parameters such as voltage step, pulse amplitude, SW frequency and the resting time have been also optimized. The optimized parameters are shown in Table 1.

Interferences studies

The electroactive compounds that are present in the real samples might be a potential interference during the electrochemical determination of the analytes. Hence, the performance of the proposed modified electrode toward detection of Pb^{2+} and Hg^{2+} ions was elvaluated in the presence of some potentially interfering ions of real samples.

SWASV were carried out in a solution containing 1.0 nM Pb^{2+} and Hg^{2+} ions in the absence/presence of various concentrations of each interference substances. The tolerance limit was taken as the maximum concentration of the interference elements, which caused a ±5% relative error or more. Interference impact of some anions and cations including Li^{+}, Na^{+}, NH_4^{+}, Ag^{+}, Mg^{2+}, Ba^{2+}, Sr^{2+}, Mn^{2+}, Cd^{2+}, Cu^{2+}, Ni^{2+}, Ca^{2+}, Al^{3+}, Bi^{3+}, As^{3+}, I^{-}, Br^{-}, NO_2^{-}, NO_3^{-}, SO_4^{2-}, and ClO_4^{-} were investigated. The obtained results as shown in Table 2, demonstrated that these external substances have no

Table 1 — The obtained results of the instrumental parameters

Instrumental parameter	Unit	Range studied	Optimum value
Voltage step	mV	1–10	5.0
Pulse amplitude	mV	10–150	100
SW frequency	Hz	10–100	50
Resting time	sec	0–60	10

Table 2 — Interference levels for some tested ions in simultaneous determination of 1.0 nM Pb^{2+} and Hg^{2+}

Interference Ions	Interference/ analyte ratio
Ni^{2+}, Li^{2+}, Al^{3+}, SO_4^{2-}	>100
Mn^{2+} , Ag^{+}, Mg^{2+}, Ni^{2+}, Cd^{2+}, Ba^{2+}, Cu^{2+}	>250
Na^{+}, Ca^{2+}, NO_3^{-}, SO_4^{2-}	>400
NH_4^{+}, Sr^{2+} Bi^{3+}, As^{3+}, I^{-}, Br^{-}, NO_2^{-}, ClO_4^{-}	>500

interference on the stripping current of Pb^{2+} and Hg^{2+} ions (until > 500 folds). Hence, the Co_3O_4-CeO_2-ZnO/CPE can be applied for the determination of Pb^{2+} and Hg^{2+} ions in real samples containing different ions.

nalytical performance of Co_3O_4-CeO_2-ZnO/CPE for determination of Pb^{2+} and Hg^{2+}

Under the optimum condition, SWV were recorded for different concentration of Pb^{2+} and Hg^{2+} on the Co_3O_4-CeO_2-ZnO/CPE. When concentrations of the both analytes were simultaneously increased, two separated stripping peaks with two linear ranges of 0.27–18.42 nM and 0.42–31.30 nM for Pb^{2+} and Hg^{2+} were obtained respectively. The linear regression equations of Pb^{2+} and Hg^{2+} and coefficients of determination were Ipa = $1.1551C_{Pb}$ + 0.2839 (R^2=0.9986) and Ipa = $0.4988C_{Hg}$ + 0.319 (R^2=0.9986), respectively (Fig. 4a and 4b). LOD of the modified electrode was calculated based on three times of standard deviation of the blank signals to calibration slope ($3S_b$/m). LODs were calculated 0.054 and 0.097 nM for Pb^{2+} and Hg^{2+}, respectively.

For individual determination of each analyte, the concentration of Hg^{2+} was kept constant in 3.0 nM while concentration of Pb^{2+} was changed from 0.27 to 18.42 nM (Fig. 5a), and in the other samples, the concentration of Pb^{2+} was kept constant in 3.0 nM while concentration of Hg^{2+} was changed from 0.42 to31.30 µg L^{-1} (Fig. 5b).

It can be seen that their stripping peak currents rose linearly for Pb^{2+} and Hg^{2+} with the following linear regression equations and coefficient of determination:

Pb^{2+} Ipa = $1.1567C_{Pb}$ + 0.2624 R^2 = 0.9983 … (1)

Hg^{2+} Ipa = $0.4983C_{Hg}$ + 0.3032 R^2 = 0.9987 … (2)

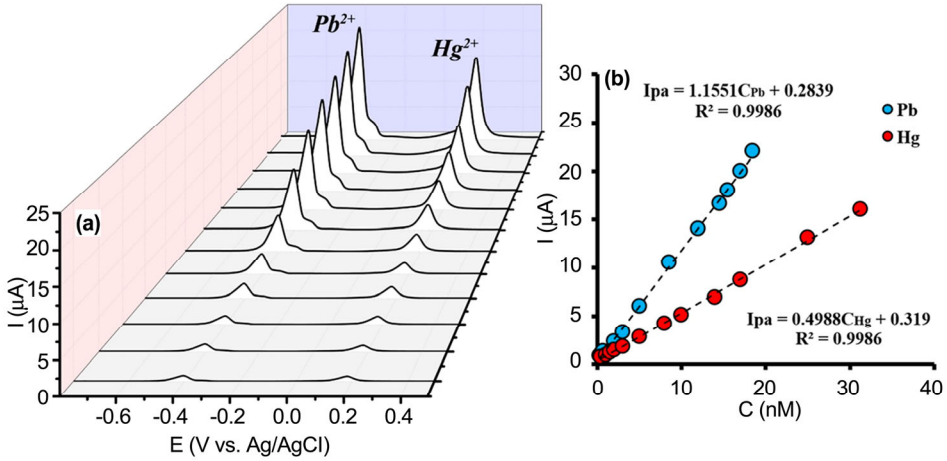

Fig. 4 — (a) SW voltammograms using Co_3O_4-CeO_2-ZnO/CPE for simultaneous determination of different concentrations of Pb^{2+} (0.27–18.42 nM) and Hg^{2+} (0.42–31.30 nM) under optimum condition. (b) Calibration plot of the voltammetric currents as a function of the analytes concentrations.

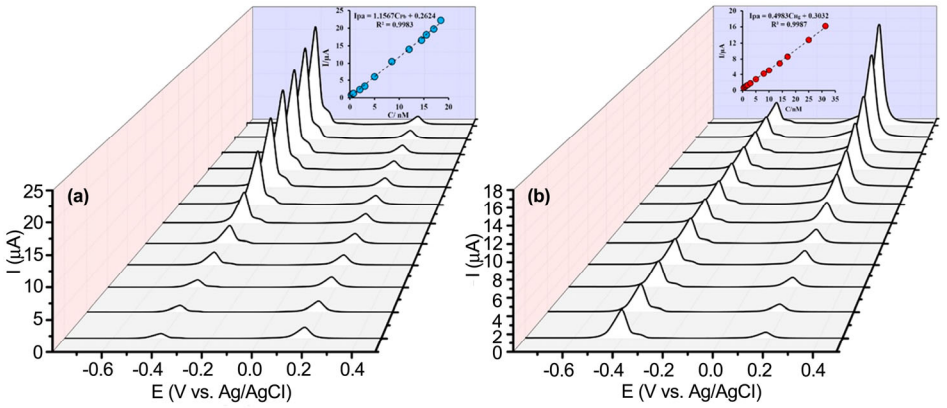

Fig. 5 — SW voltammograms using Co_3O_4-CeO_2-ZnO/CPE for (a) different concentrations of Pb^{2+} (0.27–18.42 nM) in the presence constant concentration of 3.00 nM Hg^{2+}, (b) different concentrations of Hg^{2+} (0.42–31.30 nM) in the presence constant concentration of 3.00 nM Pb^{2+}. Insets illustrate calibration plot of the voltammetric currents as a function of the analytes concentrations.

Table 3 — Results for Pb^{2+} and Hg^{2+} determination (nM) in Spice samples under the optimum conditions

No.	Spice sample	Analyte	Found	AAS
1	Cinnamon	Pb^{2+}	154.1	158.9
		Hg^{2+}	87.4	85.3
2	Hot pepper	Pb^{2+}	64.3	67.1
		Hg^{2+}	53.1	55.9
3	Turmeric	Pb^{2+}	215.1	213.0
		Hg^{2+}	42.5	39.4
4	Black pepper	Pb^{2+}	264.4	260.8
		Hg^{2+}	26.2	26.4
5	Curry	Pb^{2+}	232.0	236.7
		Hg^{2+}	86.2	85.3
6	Ginger	Pb^{2+}	151.2	156.0
		Hg^{2+}	3.0	2.5
7	Black pepper	Pb^{2+}	38.4	35.2
		Hg^{2+}	57.4	55.4
8	Pepper	Pb^{2+}	54.7	57.0
		Hg^{2+}	165.4	160.2
9	Cinnamon	Pb^{2+}	17.4	18.8
		Hg^{2+}	2.3	2.5
10	Green cumin	Pb^{2+}	92.2	94.2
		Hg^{2+}	29.3	27.3
11	Green Cardamom	Pb^{2+}	80.3	82.1
		Hg^{2+}	55.4	57.4
12	Turmeric	Pb^{2+}	122.4	119.8
		Hg^{2+}	27.0	27.9
13	Hot pepper	Pb^{2+}	50.2	49.7
		Hg^{2+}	3.0	2.5
14	Turmeric	Pb^{2+}	234.8	238.1
		Hg^{2+}	108.3	109.8
15	Black pepper	Pb^{2+}	200.5	198.5
		Hg^{2+}	2.8	2.5
16	Green cumin	Pb^{2+}	60.6	59.4
		Hg^{2+}	598.8	594.3
17	Curry	Pb^{2+}	322.4	319.7
		Hg^{2+}	127.0	123.8
18	Ginger	Pb^{2+}	105.2	107.2
		Hg^{2+}	52.9	55.9
19	Black cumin	Pb^{2+}	93.6	97.1
		Hg^{2+}	32.6	35.9
20	Curry	Pb^{2+}	522.6	425.5
		Hg^{2+}	444.6	441.6
21	Curry	Pb^{2+}	148.6	145.9
		Hg^{2+}	209.2	212.6
22	Clove	Pb^{2+}	55.5	53.6
		Hg^{2+}	23.5	22.0

The comparison of the calibration curves of Pb^{2+} and Hg^{2+} in both individual or simultaneous determination shows that two analytes have no interfere with each other and the stripping current values are entirely similar at same concentrations. Hence, Co_3O_4-CeO_2-ZnO/CPE can be successfully applied for the simultaneous determination of Pb^{2+} and Hg^{2+} in aqueous solution.

Repeatability, reproducibility, and stability of Co_3O_4-CeO_2-ZnO/CPE

In order to investigate the applicability of proposed electrode the repeatability, reproducibility and stability of Co_3O_4-CeO_2-ZnO/CPE was tested in the optimum conditions. The proposed sensor showed excellent repeatability (n = 10) with an RSD% of 2.2% and 1.9% for stripping peak currents of 1.0 nM Pb^{2+} and Hg^{2+}, respectively. The reproducibility of Co_3O_4-CeO_2-ZnO/CPE was also investigated using preparation of ten electrochemical sensors in the same procedure. The RSD were calculated 2.9% and 2.6% for of 1.0 nM Pb^{2+} and 1.0 nM Hg^{2+} respectively. The stability of the proposed electrochemical sensor was investigated by detecting the SWASV responses of the electrode. The response of electrode for 1.0 nM of Pb^{2+} and Hg^{2+} retained 95.4 and 95.6% of its initial stripping response after a period of 21 days. The results indicate that the Co_3O_4-CeO_2-ZnO/CPE has excellent repeatability, reproducibility, and long-term stability.

Analysis of spices sample

Several tests were carried out in order to determination of Pb^{2+} and Hg^{2+} in different spices samples. As it can be seen in Table 3, the results of the measurements are comprised to those obtained by Atomic absorption spectroscopy (AAS) method which confirmed the accuracy and reliability of the method. Hence the proposed method can be used for individual and simultaneous detection of Pb^{2+} and Hg^{2+} in different spices samples. The results showed that the obtained data of proposed method are in good agreement with the reference method. Linear range and detection limit of the presented method was comprised with some recently reported methods (Table 4).

Table 4 — Comparison of linear range and DL of the some recently suggested electrodes for the determination of Pb^{2+} and Hg^{2+}

Electrode	Linear range (nM)		DL (nM)		Refs.
	Pb^{2+}	Hg^{2+}	Pb^{2+}	Hg^{2+}	
PPh_3/MWCNTs/IL/CPE	0.01–150.0	0.01–150.0	0.06	0.09	[6]
IL/Gr/L/CPE	1.25–200.0	1.25–200.0	0.45	0.39	[7]
EDTA bonded conducting polymer modified electrode	0.75–100.0	0.75–100.0	0.60	0.50	[52]
Schiff base/MWCNT/CPE	2.00–700.0	2.00–700.0	0.06	0.09	[53]
$[Ru(bpy)_3]^{2+}$-GO modified Au electrode	50.0–250.0	100.0–1200.0	1.41	1.60	[54]
Co_3O_4.CeO_2.ZnO /CPE	0.27–18.42	0.42–31.30	0.054	0.097	This work

Conclusions

This study provides a new modified carbon paste electrode based on Co_3O_4-CeO_2-ZnO tri-metallic nanocomposite for determination of Pb^{2+} and Hg^{2+} ions in aqueous solution and different kind of real samples. The obtained results suggest that Co_3O_4-CeO_2-ZnO nanocomposite is better than some other modifier of CPE for the electrochemical determination of heavy metals ions. The experimental results showed that the stripping peak currents were proportional to the concentration of Pb^{2+} and Hg^{2+} ions in the range of 0.27–18.42 and 0.42–31.30 nM with DLs of 0.054 and 0.097 nM, respectively. Hence, the proposed modified electrode can be used long term, providing a low detection limit (sub-nano molar), high selectivity, reproducibility, repeatability for determination of both analytes. The electrochemical sensor could also be renewed quickly and easily by mechanical polishing with a filter paper whenever needed. Consequently, the results showed the studied method would be a promising method to use in routine analytical applications.

Acknowledgement

The authors gratefully appreciate the hard work of the staff of Razi Lab Complex of Islamic Azad University, Science and Research Branch.

References

1 Tadayon F & Sepehri Z, *RSC Advances*, 5 (2015) 65560.
2 Zhu C, Yang G, Li H, Du D & Lin Y, *Anal Chem*, 87 (2015) 230.
3 Walcarius A, Minteer S D, Wang J, Lin Y & Merkoci A, *J Mater Chem*, B1 (2013) 4878.
4 Chen A & Chatterjee S, *Chem Soc Rev*, 42 (2013) 5425.
5 Sanghavi B J, Wolfbeis O S, Hirsch T & Swami N S, *Microchim Acta*, 182 (2015) 1.
6 Bagheri H, Afkhami A, Khoshsafar H, Rezaei M & Shirzadmehr A, *Sens Actu B*, 186 (2013) 451.
7 Bagheri H, Afkhami A, Khoshsafar H, Rezaei M, Sabounchei S J & Sarlakifar M, *Anal Chim Acta*, 870 (2015) 56.
8 Bagheri H, Shirzadmehr A & Rezaei M, *J Mol Liq*, 212 (2015) 96.
9 Bagheri H, Shirzadmehr A & Rezaei M, *Ionics*, 22 (2016) 12.
10 Rezaei M, *Anal Bio Electrochem*, 8 (2016) 287.
11 Khoshsafar H, Bagheri H, Rezaei M, Shirzadmehr A, Hajian A & Sepehri Z, *J Electrochem Soc*, 163 (2016) B422.
12 Shirzadmehr A, Rezaei M, Bagheri H & Khoshsafar H, *Inter J Env Anal Chem*, 96 (2016) 929.
13 Bagheri H, Hajian A, Rezaei M & Shirzadmehr A, *J Hazard Mater*, 324 (2017) 762.
14 Tok A I Y, Boey F Y C, Dong Z & Sun X L, *J Mater Process Technol*, 190 (2007) 217.
15 Kaviyarasu K, Sajan D, Selvakumar M S, Thomas S A & Anand D P, *J Phys Chem Solids*, 73 (2012) 1396.
16 Liu B, Liu Y, Li C, Hu W, Jing P, Wang Q & Zhang J, *Appl Catal B*, 127 (2012) 47.
17 Yan J, Wei T, Qiao W, Shao B, Zhao Q, Zhang L & Fan Z, *Electrochim Acta*, 55 (2010) 6973.
18 Park S & Kim S, *Electrochim Acta,* 89 (2013) 516.
19 Wu F, Ma X, Feng J, Qian Y & Xiong S, *J Mater Chem*: *A*2, (2014) 11597.
20 Yan C, Chen G, Zhou X, Sun J & Lv C, *Adv Funct Mater*, 26 (2016) 1428.
21 Lin H K, Wang C B, Chiu H C & Chien S H, *Catal Lett*, 86 (2003) 63.
22 Haneda M, Kintaichi Y, Bion N & Hamada H, *Appl Catal B: Environ*, 46 (2003) 473.
23 Mu J, Zhao X, Li J, Yang E C & Zhao X J, *Mater Sci Eng,* C74 (2017) 434.
24 Senanayake S D, Stacchiola D & Rodriguez J A, *Acc Chem Res*, 46 (2013) 1702.
25 Martinez-Arias M, Fernandez-Garcia M, Galvez O, Coronado J M, Anderson J A, Conesa J C, Soria J & Munuera G, *J Catal*, 195 (2000) 207.
26 Li R, Yabe S, Yamashita M, Momose S, Yoshida S, Yin S & Sato T, *Solid State Ionics*, 151 (2002) 235.
27 Kumar S, Kim Y J, Koo B & Lee C G, *J Nanosci Nanotechnol*, 10 (2010) 7204.
28 Azarang M, Shuhaimi A, Yousefi R & Sookhakian M J, *Appl Phys*, 116 (2014) 084307.
29 Kumar KY, Muralidhara HB, Nayaka YA, Balasubramanyam J & Hanumanthappa H, *Powder Technol*, 246 (2013**)** 125.
30 Wang X B, Cai W P, Liu S W, Wang G Z, Wua Z K & Zhao H J, *Colloids and Surfaces A: Physicochem Eng Aspects*, 422 (2013) 199.
31 Jana T, Pal A & Chatterjee K, *J Alloys Compd*, 653 (2015) 338.
32 Kaur J, Bhukal S, Gupta K, Tripathy M, Bansal S & Singhal S, *Mater Chem Phys*, 177 (2016) 512.
33 Subhan M A & Ahmed T, *Spectrochim Acta Part A*, 129 (2014) 377.
34 Afkhami A, Madrakian T, Sabounchei S J, Rezaei M, Samiee S & Pourshahbaz M, *Sens Actuators B*, 161 (2012) 542.
35 Scoullos M, Vonkeman G H, Thornton I & Makuch Z, *Mercury—Cadmium—Lead Handbook for Sustainable Heavy Metals Policy and Regulation*, (Springer Science & Business Media, vol 31) 2012.
36 Afkhami A, Madrakian T & Siampour H, *J Hazard Mater*, 138 (2006) 269.
37 Cornard J P, Caudron A & Merlin J C, *Polyhedron,* 25 (2006) 2215.
38 Moreno R G, Oliveira E de, Pedrotti J J & Oliveira P V, *Spectrochim Acta B,* 57 (2002) 769.
39 Torres AG de & Pavón J C, *J Anal At Spectrom,* 8 (1993) 705.
40 Debrah E, Denoyer E R & Tyson J F, *J Anal At Spectrom*, 11 (1996) 127.
41 Abbasi S, Bahiraei A & Abbasai F, *Food chem*, 129 (2011) 1274.
42 Afkhami A, Bagheri H, Shirzadmehr A, Khoshsafar H & Hashemi P, *Electroanal,* 24 (2012) 2176.
43 Schumacher P D, Fitzgerald K A, Schenk J O & Clark S B, *Anal Chem*, 83 (2011) 1388.
44 Wei Y, Gao C, Meng F L, Li H H, Wang L, Liu J H & Huang X J, *J Phys Chem C*, 116(1) (2012) 1034.
45 Mafa P J, Idris A O, Mabuba N & Arotiba O A, *Talanta*, 153 (2016) 99.
46 Liu J, Zhu G, Chen M Ma X & Yang J, *Sens Actuators B: Chem*, 234 (2016) 84.

47 Xie Y L, Zhao S Q, Ye H L, Yuan J, Song P & Hu S Q, *J Electroanal Chem*, 757 (2015) 235.
48 Adarakattia P S, Gangaiah V & Siddaramanna A, *Mater Sci Semicon Proc*, 84 (2018) 157.
49 Zuo Y, Xu J, Jiang F, Duan X, Lu L, Xing H, Yang T, Zhang Y, Ye Guo & Yu Y, *J Electroanal Chem*, 801 (2017) 146.
50 Liu Z G, Chen Xing, Liu J H & Huang X J, *Electrochem Commun*, 30 (2013) 59.
51 Ping J, Wu J, Ying Y, Wang M, Liu G & Zhang M, *J Agric Food Chem*, 59 (2011) 4418.
52 Rahman M A, Won M S & Shim Y B, *Anal Chem*, 75 (2003) 1123.
53 Afkhami A, Bagheri H, Khoshsafar H, Saber-Tehrani M, Tabatabaee M & Shirzadmehr A, *Anal Chim Acta*, 746 (2012) 98.
54 Gumpu M B, Veerapandian M, Krishnan U M & Rayappan J B B, *Talanta,* 162 (2017) 574.